

# Stretching strain - effective “negative” pressure in Lead selenide nanolayers

A.M. Pashaev<sup>1</sup>, O.I. Davarashvili<sup>2</sup>, M. I. Erukashvili<sup>2</sup>, Z. G. Akhvlediani<sup>2,3</sup>,  
L.P.Bychkova<sup>2</sup>, R.G. Gulyaev<sup>2</sup>, V.P. Zlomanov<sup>4</sup>

<sup>1</sup>National Aviation Academy, Baku A2-1045, Azerbaijan

<sup>2</sup>Iv. Javakhishvili Tbilisi State University, Tbilisi 0128, Georgia

<sup>3</sup>E.Andronikashvili Institute of Physics, Tbilisi 0186, Georgia

<sup>4</sup>M. Lomonosov Moscow State University, Moscow 119899, Russia

**Abstract.** *The PbSe layers were grown on KCl substrates by molecular epitaxy with a “hot wall”, the range of layers thickness was from 20 to 2000nm. Special emphasis was given to the nanolayers < 200nm thick. The approximation of the tangential lattice constant of the layers to that of the substrate as the layers thickness decreases points to the fact that the strain (at tensile deformation) in the layers is associated with the mismatch between layer and substrate lattice constants. The increases in the forbidden gap width is associated with stretching of layers as well. The increase in the tangential lattice constant and the forbidden gap width in IV-VI semiconductors fit well the notion of “negative” pressure.*

**Key words:** nanolayer, lead selenide, “negative” pressure, tangential lattice constant, forbidden gap width.

## I. INTRODUCTION

Strained layers in semiconductor structures are successfully employed for increasing the efficiency of radiation sources and fine tuning of their frequency over a wide spectral range [1].

The range of application of strained semiconductor layers extend significantly when these layers are grown on heterogeneous substrates with the mismatch of  $>0.01$ . In this case, there appear new possibilities for designing of high-sensitivity and high-temperature photo detectors, especially in the infrared (IR) spectral region, on the basis, for instance, of lead selenide and its solid solutions. The layers that are not compressed, but stretched by the substrate are of great interest. In this case, the forbidden gap width of IV-VI semiconductors increases. The following interesting scheme appears: when lead selenide layers are doped with impurities such as Cr, In and Yb, under tensile deformation their levels shift to the forbidden gap, they compensate electrically active nonstoichiometric defects, and the concentration of current carriers can decrease significantly. As a result, in the narrow-gap semiconductor, the quasi-dielectric state is realized with preserving the character of band-to-band transitions [2]. The abovementioned conditions correspond to the effective “negative” pressure in the IV-VI semiconductors.

The physics of “negative” pressure and crystals lays the groundwork for strongly non-equilibrium materials science, when the layer can be as an efficient getter of the defects decreasing entropy of layers. This problem is likely to become the subject of much concentrated attention in materials nanotechnology.

This article deals with the two basic issues of formation of quasi-dielectric state: the realization of “negative” pressure and the corresponding increase in the forbidden gap width in lead selenide. The results of these investigations also will be employed for designing of IR lasers, piezoresistors and local thermoelectric devices. This paper is organized in the following way. In Sec. II we introduce the experimental methods. The results of measurements and discussion are given in Sec. III. Finally, in Sec. IV we present the conclusions.

## II. EXPERIMENTAL METHODS

For stretching the lead selenide layers, they were grown on the substrates with a higher lattice constant, for instance, KCl ( $a=6.290 \text{ \AA}$ ), than that of PbSe ( $a=6.126 \text{ \AA}$ ), the initial mismatch made up  $f = 0.026$  [3]. Due to the relaxation of strains, in practice, it is difficult to achieve the deformation at the level of initial mismatch. It is important to form the conditions for the maximum unrelaxed state by generating the barriers to the movement of dislocations, which just accumulate the elastic energy of layers. Various physical and technological factors could be the barriers of this type. They include the high concentration of nonstoichiometric defects, and the control of epitaxy temperature [4].

The PbSe layers on KCl (100) substrates were grown by epitaxy with a “hot wall”. Polycrystalline lead selenide was the source of epitaxy. During its synthesis, the lead oxide film was preliminarily reduced in hydrogen by heating up to  $700 \text{ }^\circ\text{C}$ , and then the melted lead was filtered through a capillary tube. Purified components of selenium and lead were sealed in a quartz ampoule and heated up to  $900\text{-}1000^\circ\text{C}$  for 4 hours and quenched in the air.

The temperature of the PbSe source of epitaxy was within the range of  $450\text{-}510^\circ\text{C}$ . According to [5], the pressure of saturated PbSe vapor varied over the range of  $2 \cdot 10^{-5}\text{-}7 \cdot 10^{-5} \text{ mm Hg}$ , which allowed us to maintain the layer growth rate in the range from 0.5 to 10nm/s. In this range, the growth rate increased 3-fold when the distance between the open end of the quartz ampoule (containing the source) and the substrate decreased from 12 mm to 1mm and increased 2 times more when the source temperature increased from  $470\text{ to }510 \text{ }^\circ\text{C}$ . The

temperature of the KCl substrate was in the range of 240 - 300°C. The KCl substrates treated immediately before epitaxy (with the maximum mismatch with the plane (100) less than 20') by cutting off were heated up at the temperature higher than the temperature of epitaxy by 100°C for an hour.

**Table 1 . Tangential lattice constants, thickness and relative mismatch-deformations for epitaxial PbSe layers grown on KCl (100) substrates (d= 20-2000 nm)**

No	Layer	Substrate temperature T, °C	Source temperature T, °C	Time of layer growth t, s	Tangential lattice constant $a_t$ , Å	Layer thickness d, nm	Layer growth rate $v$ , nm/s	Relative mismatch-deformation $\epsilon = \frac{a_t - a_{PbSe}}{a_{PbSe}} \cdot 10^2$
1	SL-69	240	510	3600	6.126(4)	1830	0.5	0
2	SL -216	240	450	300	6.136(4)	193	0.6	0.163
3	SL -237	280	470	90	6.142(1)	157	1.8	0.261
4	SL -277	240	470	30	6.149(0)	181	6.0	0.375
5	SL -241	300	470	80	6.162(4)	101	1.8	0.586
6	SL -258	300	470	77	6.172(0)	83	1.1	0.751
7	SL -255	300	470	75	6.177(4)	68	0.9	0.833
8	SL -262	300	470	67	6.188(2)	52	0.8	1.012
9	SL -185	240	450	360	6.203(3)	41	0.1	1.257
10	SL -180	240	450	315	6.211(3)	29	0.1	1.379
11	SL -177	300	450	330	6.219(5)	22	0.07	1.518

The “negative” pressure in the layers was assessed through the deformations, which in turn were determined by measuring the tangential lattice constants by X-ray diffraction patterns of reflection from the crystallographic plane (400) in the mode of  $\theta - 2\theta$  scanning. The tangential lattice constants were determined by the formula:

$$a_t = \lambda / 2 \sin \theta \cdot \sqrt{(h^2 + k^2 + l^2)} = 2\lambda / \sin \theta \quad (1)$$

Where  $\lambda$  is the X-ray radiation wavelength;  $\theta$  is the Bragg diffraction angle; h, k and l are the Miller indices. The deformation  $\epsilon$  in the epitaxial layers with respect to the PbSe monocrystal was determined as follows:

$$\epsilon = (a_t - a_{PbSe}) / a_{PbSe} \quad (2)$$

The layers thickness was determined using the X-ray method by measuring the reflection from multiple planes (200) and (400) with and without the layer.

The forbidden gap width was assessed with optical transmission recorded by using the double-beam prism – diffraction spectrophotometer SPECORD – 75IR in the wavelength range of 2.5-25  $\mu\text{m}$ .

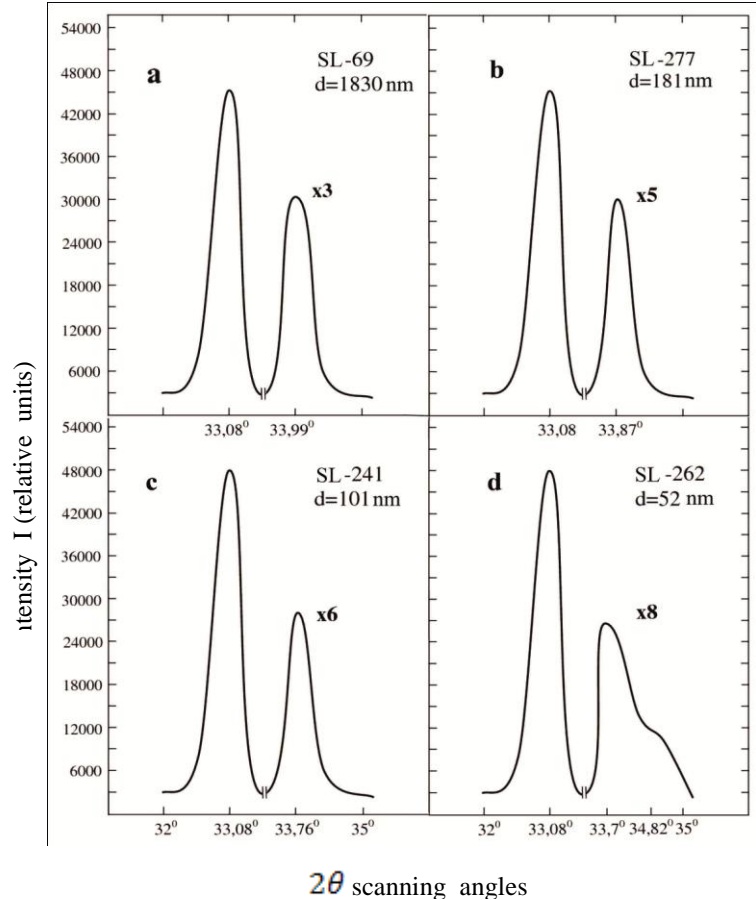


**Fig 1. Diffraction patterns of  $\theta - 2\theta$  scanning of thin epitaxial PbSe layers of different thickness; reflection plane (200),  $2\theta = 33.08^\circ$  corresponds to the KCl substrate**

III. RESULTS AND DISCUSSION

Since the deformations in the layers decreased as the layers thickness increased, they were studied mainly at a thickness of less than 200nm . At temperature <200°C, the layers grew amorphous, and hence their growth proceeded from the temperature of 240°C, and the time of growth decreased gradually.

In Table 1 are listed the growth conditions for some epitaxial layers, their thickness, the lattice constants and corresponding deformations. It is obvious from Table 1 that, at the same temperature of the source of epitaxy of 470°C, while the growth time changed from 80 to 67s , the layers thickness changed from 101 to 52 nm. Such changes in the layers thickness at insignificant variations in the growth time point to the delay in the initiation of growth. This delay actually turned to be the first stage of slow growth – nucleation and merging of nuclei-islands. This process of formation of a uniform layer took 60 s, and then followed the second stage of fast gradual growth . The corresponding deformations in the layers with respect to the PbSe monocrystal made up  $0.586 \cdot 10^{-2} - 1.012 \cdot 10^{-2}$ .

Layers < 40nm thick were grown under heating up of the substrate from the rear by a convalescent bulb. In this case the growth rate of the layers decreased significantly, and it was more convenient to control their thickness. By those layers, the maximum strain - “negative” pressure realized in them was determined. For instance, for layer SL-177 with the tangential lattice constant  $a_t = 6,219(5) \text{ \AA}$  and the corresponding deformation  $\epsilon = 1.518 \cdot 10^{-2}$ , the strain was

$$\sigma = \frac{E}{1 - \nu} \epsilon = 1.2 \cdot 10^{10} \text{ dyne/cm}^2 = 12 \text{ kbar}$$

(the modulus of elasticity is  $E = 5 \cdot 10^{11} \text{ dyne/cm}^2$ , the Poisson’s ratio is  $\nu = 0.38$ ) and was developed despite of appearance of disturbances – textures (Fig.1d) . In Fig. 1(a,b,c,d) are shown also the X-ray diffraction patterns of  $\theta$ - $2\theta$  scanning for the layers of different thickness.

As the layers thickness decreases, the X-ray peaks of the layers shift to the peak of the substrate, i.e. the tangential lattice constants increase. It is noteworthy that the intensity of reflection from unstrained layer SL-69 made up 90% of the intensity of reflection from the PbSe monocrystal. The diffraction patterns given in Fig. 1(a,b,c,d) show that the deformations in the layers were determined by the mismatch between the lattice constants of the layer and the substrate, and not by the discrepancy between the thermal expansion coefficients (TEC). If the deformations had been associated with the discrepancy between the TECs, owing to significant compression of the KCl substrate, during cooling the PbSe layer should have been compressed as well, and its lattice constant should have been  $< 6.126 \text{ \AA}$  . However, up to the angles of  $2\theta = 35^\circ$  corresponding to the lattice constant  $6.0 \text{ \AA}$ , there was detected no signal: the mismatch between the lattice constants of the layer and the substrate exceeded the change in the lattice constant of the layer because of the discrepancy between the TECs. This means that the deformations revealed in thin layers stretched the layer, i.e. the effective “negative” pressure was realized.

Another indicator of the realization of “negative” pressure in strained epitaxial layers of IV-VI semiconductors is the increase in the forbidden gap width with the growing deformation in them. We have elaborated the methods of determination of the forbidden gap width of the layers of different thickness, including nanolayers, by optical transmission [6]. At the first stage, by optical transmission spectra, sequential determination of the refractive index, and the reflection and absorption coefficients was performed. Then, for direct band-to-band transitions characteristic of IV-VI semiconductors, the forbidden gap width was determined by straightening of the squared product of the interband absorption coefficient and the photon energy  $(ah\nu)^2 = f(h\nu)$  and the obtained results were compared with the ones obtained by approximation in accordance with the second-type straightening  $\alpha^2 = f(h\nu)$ .

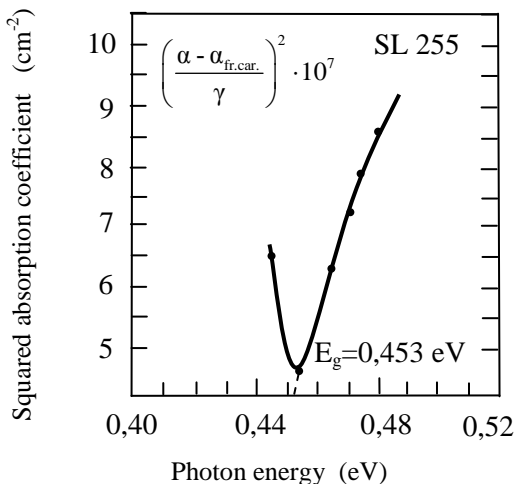


Fig 2a. Squired absorption coefficient dependence on photon energy :  $\alpha^2 = f(h\nu)$

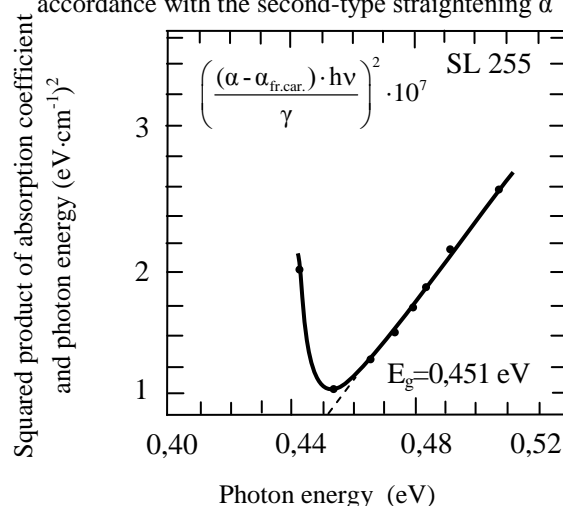


Fig 2b. Squared product of absorption coefficient and photon energy dependence on photon energy :  $(ah\nu)^2 = f(h\nu)$

The spectra of epitaxial layers <700nm thick generally showed a monotonic increase with a small slope as the wavelength increased. In this case, as well as in the case of thick layers in the spectra of which interference peaks were revealed, such spectra were processed by a model of the Fabry-Perot interferometer. Taking the epitaxial PbSe layer as a resonator the ends of which are the boundaries with the substrate and the air, the model considers the interference as the one damping in the wave layer under multiple reflection from the resonator boundaries. The magnitude of the transmission coefficient through the layer is the following:

$$T = (1 - r_1^2)(1 - r_2^2) \exp(2\beta_i \cdot d) / [(1 - R)^2 + 4R \sin^2 \beta \cdot d] \quad (3)$$

Where  $r_1 = N_{PbSe} - N_{air} / N_{PbSe} + N_{air}$  is the amplitude value of reflection coefficient at the PbSe/air interface;  $r_2 = N_{PbSe} - N_{KCl} / N_{PbSe} + N_{KCl}$  is the amplitude value of reflection coefficient at the PbSe (layer) - KCl (substrate) interface,  $R = r_1 r_2 \exp(2\beta_i \cdot d)$ ,  $\beta = 2\pi N / \lambda$ ,  $\beta_i = -\alpha / 2$  is the absorption coefficient.

Extrapolating the values of the refractive index determined by interference peaks, for instance, for layer

SL-69 1.83μm thick, the values  $r_1$  and  $r_2$  in the short-wavelength region were obtained [6]. The obtained values of  $r_1$  and  $r_2$  were substituted into the equation for determination of the absorption coefficient  $\alpha$  through  $y = \exp(-\alpha d)$ :

$$T(r_1 r_2)^2 y^2 - (1 - r_1^2)(1 - r_2^2) y + \left( 2Tr_1 r_2 - 4Tr_1 r_2 \sin^2 \frac{2\pi N d}{\lambda} \right) y + T = 0 \quad (4)$$

Because of the high concentration of current carriers ( $\sim 10^{19} \text{cm}^{-3}$ ) in the epitaxial layers, the absorption by free carriers is high, and it could be quite significant in the region of eigen absorption as well. Hence the straightening of squared absorption coefficients is performed by the relationship  $(\alpha - \alpha_{fr.car})^2 = f(h\nu)$ .

**Table 2. Data for the tangential lattice constants, deformations (strains) and corresponding forbidden gap width in PbSe layers.**

No	Layer	Layer thickness d, nm	Tangential lattice constant $a_\tau$ , Å	Relative mismatch-deformation $\epsilon = \frac{a_\tau - a_{PbSe}}{a_{PbSe}}$	Strain $\sigma = \frac{E}{1-\nu} \epsilon$ , kbar	$E_g$ , eV
1	SL-69	1830	6.126(4)	0	0	0.286
2	SL-277	181	6.149(0)	0.0038	3,1	0.340
3	SL -304	119	6.154(8)	0.0047	3,8	0.355
4	SL -255	68	6.177(4)	0.0083	6,7	0.454

The quantity  $\alpha - \alpha_{fr.car}$  corresponds to interband absorption and characterizes its edge, especially in thin layers where,

along with the high concentration of current carriers, a significant decrease in the relaxation time is observed.

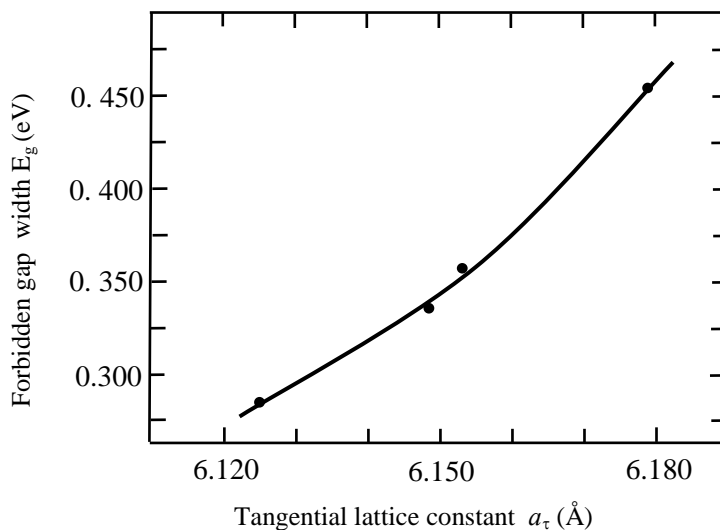


**Fig 3 Dependence of the forbidden gap width of PbSe layers on the tangential lattice constant**

As at high concentrations of current carriers the transitions between band edges are impossible because of the Burstein effect, for determination of the forbidden gap width, the straightening of function

$$\left[ \frac{1}{\gamma} (\alpha - \alpha_{fr.car.}) \right]^2 = f(h\nu)$$
 is performed. In this expression,  $\frac{1}{\gamma}$  accounts for degeneration, and the

dependence of this factor on the forbidden gap width and the Fermi level  $E_F$  is given in Ref. [7]. Figure 2, a, b shows the relationships  $(\alpha' h\nu)^2 = f(h\nu)$  and  $(\alpha')^2 = f(h\nu)$  for layer SL-255 68 nm thick with the tangential lattice constant  $a_t = 6.177(4) \text{ \AA}$ . Attention was paid to the fact that, in the particular spectrum region of 2.5-5.0  $\mu\text{m}$ , the interband absorption  $\alpha = \alpha_{exp.} - \alpha_{fr.car.}$  was positive, and, for direct band-to-band transitions, it varied in the interval from  $3 \cdot 10^3$  to  $10^4 \text{ cm}^{-1}$ . Proceeding from this point, the relationships  $(\alpha')^2 = f(h\nu)$  and  $(\alpha h\nu)^2 = f(h\nu)$  were constructed [8]. In Table 2 are presented data on the forbidden band gap at  $T=300\text{K}$  with corresponding tangential lattice constants and deformations. The value  $4.42 \text{ cm}^2/\text{V}\cdot\text{s}$  was taken as the average mobility of current carriers, while, in the calculation of coefficient  $\gamma$ , the values  $E_{g0}=0.286 \text{ eV}$  and  $E_F=0.03 \text{ eV}$  were used. As is evident from Fig. 2, a, b, the straightening of both types yielded for  $E_g \sim 0.453$  and  $0.451 \text{ eV}$ , respectively. These values differed from the  $E_g = 0.454 \text{ eV}$  determined by the minimum of the relationships given in Fig. 2, a, b within  $0.003 \text{ eV}$ , which was less than the experimental error ( $\sim 0.005 \text{ eV}$ ). Proximity of the  $E_g$  values by both types of straightening could be explained by the fact that the photon energy changed only slightly at the straightening section. The  $E_g$  value increased by  $\sim 0.17 \text{ eV}$  as compared with the unstrained layer. The estimation showed that, at the given layer thickness and the sub grain size  $\sim 50 \text{ nm}$  [9,10], the increment of the forbidden gap width was determined by deformation and not by quantum effects (if effective mass in the nanolayers is not changed significantly).

Figure 3 shows the dependence of the forbidden gap width on the tangential lattice constant. The deformation

corresponding to the lattice constants of, for instance,  $6.149(0) \text{ \AA}$  - layer SL-277 and  $6.177(4) \text{ \AA}$  - layer SL-255 made up 0.004 and 0.008, respectively. It is obvious from Fig. 3 that, with growing deformation, the forbidden gap width increased more rapidly, almost twice as much, as compared with its changes in the row SL-69 – SL-277 – SL-255 (Table 2).

#### IV. CONCLUSIONS

The monocrystalline and uniform PbSe layers were grown on KCl substrates by molecular epitaxy with a “hot wall”. The dependences of the deformation on layer thickness and of the forbidden gap width on the tangential lattice constant were studied. Special emphasis was given to the nanolayers  $< 200 \text{ nm}$  thick. The deformations in the layers were determined by measuring the tangential lattice constant. It was established that with the decrease of the layers thickness the deformation (stretching) in the layers increased and, for instance, for the layer 22 nm thick the deformation  $\varepsilon$  was 0.015 and corresponding strain - 12 kbar. It was shown that deformations in the layers were connected with the mismatch between the PbSe layer and the KCl substrate (more accurately that is after strain relaxation at the layer-substrate interface). The effect of stretching of the PbSe layer – effective “negative” pressure was also revealed when the forbidden band gap was determined by studying of the optical transmission. The optical spectra were processed by a model of the Fabry-Perot interferometer. The methods of sequential determination of the index of refraction, reflection and absorption coefficients and with taking into account the degeneracy of current carriers were developed. The values of the forbidden band gap determined by the straightening of two relationships  $(\alpha')^2 = f(h\nu)$  and  $(\alpha h\nu)^2 = f(h\nu)$  coincided and were equal to  $0.454 \text{ eV}$  at the deformation  $\varepsilon = 0.008$ . In this case the increment of the forbidden band gap was  $0.17 \text{ eV}$  in comparison with the unstrained PbSe layer and on the whole this increment is determined by deformation and not by quantum effects. These investigations and the obtained results are an essential base for the creation of new IR high-sensitivity and high-temperature photo detectors, tunable lasers by optical pumping and local thermoelectric devices by doping PbSe (or other compositions of IV-VI semiconductors) nanolayers.

#### REFERENCES

- [1] A.M. Pashaev, O.I. Davarashvili, M. I. Erukashvili, R.G.Gulyaev, V. P. Zlomanov. Supercritical Nanostructures PbSe/KCl, GEN, 2011, 2, 88-93.
- [2] A.M. Pashaev, O.I. Davarashvili, V.A. Aliyev, M. I. Erukashvili, V. P. Zlomanov. Problems of Mismatch in the Heterostructures Based on IV-VI Semiconductors. In: Progress in Science and Engineering of Modern Aviation, 2009, 1, 18-20.
- [3] A.M.Pashaev, O.I.Davarashvili, Z.G.Akhvediani, M.I.Erukashvili, R.G.Gulyaev, V.P.Zlomanov. Unrelaxed State in Epitaxial Heterostructures Based on Lead Selenide. J.Mod.Phys. 2012, 3(6), 502-510.
- [4] Z. G. Akhvlediani, O.I. Davarashvili, A.M. Pashaev, M. I. Erukashvili, R. G. Gulyaev. On the Contribution of Point Defects to the Formation of Supercritical Nanostructures Based on Lead Selenide. In: Book of Abstracts of the 16<sup>th</sup> International Conference on Radiation Defects in Insulators, Beijing, 2011, 216.
- [5] V.P.Zlomanov, B.A.Popovkin, A.V. Novoselova. Determination of the Pressure of Saturated Vapor of Solid Lead Selenide. J. Inorg. Chem., 1959, 4, 12, 2661-2664.



ISSN: 2277-3754

ISO 9001:2008 Certified

International Journal of Engineering and Innovative Technology (IJET)

Volume 3, Issue 11, May 2014

- [6] A.M. Pashaev, O.I. Davarashvili, Z. G. Akhvlediani, M. I. Erukashvili, L. P. Bychkova, M.A. Dzaganian .Study on the Forbidden Gap Width of Strained Epitaxial Lead Selenide Layers by Optical Transmission. J. Mat. Sci. Eng., 2012, B2(2), 142-150.
- [7] E. Palik, D. Mitchel, J. Zemel. Magneto-Optical Studies of the Band Structure of PbS. Phys. Rev., 1964, 135A, A763-A768.
- [8] A.M. Pashaev, O.I. Davarashvili, Z.G. Akhvlediani, M. I.Erukashvili, L.P.Bychkova, M.A. Dzaganian .Interpretation of the Optical Transmission Spectra of Lead Selenide Layers with the Aim of Determination of the Width of Their Forbidden Gap .Trans. Azer.Nat.Aviation Acad. 2013, 15, 3.
- [9] A.M. Pashaev, O.I. Davarashvili, M. I. Erukashvili, R.G.Gulyaev, M.A.Dzaganian, V.P.Zlomanov. Investigation of the Degree of Dispersion of Epitaxial Lead Selenide Layers. Bull.Georg.Nat.Acad.Sci. 2011, 37(1), 3-6 .
- [10] A.M. Pashaev, O.I. Davarashvili, Z.G.Akhvlediani, M.I.Erukashvili, R.G.Gulyaev, V.P.Zlomanov .The Structure of Thin Epitaxial Layers of Lead Selenide .J.Mat.Sci.Eng., 2013, 3(2) ,117-122.